Lymphology 25 (1992) 120-130

PARTICLE CLEARANCE FROM THE CANINE PLEURAL SPACE INTO THORACIC LYMPH NODES: An Experimental Study

A.S. Pereira, N.R. Grande

Normal Morphology Unit, Abel Salazar Biomedical Science Institute, University of Oporto, Portugal

ABSTRACT

We instilled tungsten powder ($CaWO_4$) into the pleural space of the dog and studied the kinetics and distribution of particle translocation from the pleural space to the thoracic lymph nodes over 1-7 days. We found that the transport of tungsten particles to regional lymph nodes was present at day 1, and reached its peak at day 3. In situ *detection of tungsten by elemental particle analysis of lymph node sections by scanning electron microcopy complemented by light microscopy and X-ray analysis allowed precise mapping of the marker in the thoracic nodes. The first lymph nodes to become tungsten-laden was the parasternal group (day 1-3). From day 3 to 7 tungsten inclusions decreased in these parasternal nodes while moderately increasing in the remaining intrathoracic lymph nodes. Retrocardiac pleural folds containing numerous "milky spots" also accumulated prominent amounts of tungsten early after intrapleural injection of $CaWO_4$.*

These data indicate that 1) particle translocation from the pleural space to regional lymph nodes is a rapid process and is first directed to the parasternal lymph nodal subgroup; 2) particle dissemination to virtually all other lymph nodes within the thorax follows thereafter; 3) retrocardiac pleural folds contribute to the clearance of particles from the pleural space.

Many respiratory disorders involve the pleural space. This serous cavity is often infiltrated by exogenous particles, infectious agents, tumor cells and also undergoes pathologic changes with a multitude of systemic diseases (1). Current structural and physiological information envisages the pleura as having important immunologic as well as biomechanical functions. A number of recent experimental studies examining the clearance capability of the pleural space have been directed primarily to fluid and electrolyte transport as opposed to particle removal (2,3). Although several studies have previously described the anatomical pathways of drainage of the pleural space (4-7), a complete understanding of the absorption-kinetics of the pleural space is still lacking. Insight into these drainage pathways is particularly relevant in light of proposed strategies of coupling administration of cytostatic drugs with particles via the pleural space (8). Accordingly, we examined the absorption of a particulate (calcium tungstate powder or $CaWO_4$) from the canine pleural space using several anatomical methods and were able to characterize the kinetics of the arrival of $CaWO_4$ to the different subgroups of intrathoracic lymph nodes. We also noted the importance of retrocardiac pleural folds in clearing tungsten from the pleural space. Finally, we compared the findings with an earlier study from our laboratory in which

$CaWO_4$ clearance from the bronchoalveolar space was examined (9).

MATERIALS AND METHODS

Animals

Fourteen male and female adult mongrel dogs were used. The dogs were housed individually in kennels, fed standard dog food, and had unrestrained access to water. Food and water were withheld overnight before anesthesia.

Experimental protocol

Dogs were anesthetized by intravenous injection of sodium pentobarbital (40mg/kg BW). Access to the right pleural space was obtained via a thoracotomy between the fourth and fifth ribs. The parietal pleura was punctured with a rubber catheter for instillation of 5g of calcium tungstate ($CaWO_4$; Aldrich Chemical Company Inc., Milwaukee, WI USA) in 10ml saline into the pleural space. Care was taken that no injury to the visceral pleura occurred.

The dogs were divided into five groups of two dogs each that were sacrificed 1,2,3,5 and 7 days after $CaWO_4$ instillation into the pleural space. Two additional groups of two dogs each were used to control the cytological and radiological appearance of the tungsten-particulate. The dogs of the first control group were untreated; the dogs of the second control group were sham-operated; no $CaWO_4$ was instilled and they were sacrificed 7 days after surgery. All dogs were sacrificed by a lethal intravenous injection of sodium pentobarbital after radiography of the thorax. Samples of the following intrathoracic lymph nodes were collected: left and right parasternal; left and right lung hilum; left and right para-aortic; large medial lymph node (located just beneath the carina). Left and right retrocardiac pleural folds were also sampled. Each specimen was processed for 1) x-ray analysis; 2) light microscopy; 3) scanning electron microscopy.

X-ray analysis

Immediately before dog sacrifice, plain X-ray films of the thorax were obtained using a Philips Politome machine with a voltage of 50Kv and automatic focusing. After sacrifice, high resolution radiography of different thoracic structures, including lymph nodes, pleural folds, lung, and diaphragm was performed using a Siemens Mammograph in the automatic mode. The photographic film was that regularly used to examine the human breast for micro-calcifications. Nodal and pleural samples were also obtained for eight microscopy analysis and SEM.

Light microscopy

Whole lymph nodes were fixed *in toto* in formaldehyde and embedded in paraffin. Serial sections, 5μm thick were stained with hematoxylin and eosin and examined in a Zeiss Axioplan microscope. We used a semiquantitative method to compare the amount of tungsten inclusions among lymph nodal groups. The following criteria were used based on examination of 100 microscopic fields (magnification x600) chosen at random in each slide sample.

Grade 0 - No tungsten particle seen.

Grade + - Tungsten found in 1 out of 10 microscopic fields.

Grade ++ - Tungsten found in 8-9 out of 10 microscopic fields.

Grade +++ - Tungsten found in all microscopic fields.

Grade ++++ - Tungsten found both in all microscopic fields along with multiple inclusions in each tungsten positive cell.

Scanning electron microscopy

Aldehyde fixed and washed nodal and pleural samples were dehydrated in ethanol and critical-point-dried in a Balzers apparatus using carbon dioxide as the transitional fluid. The preparations were

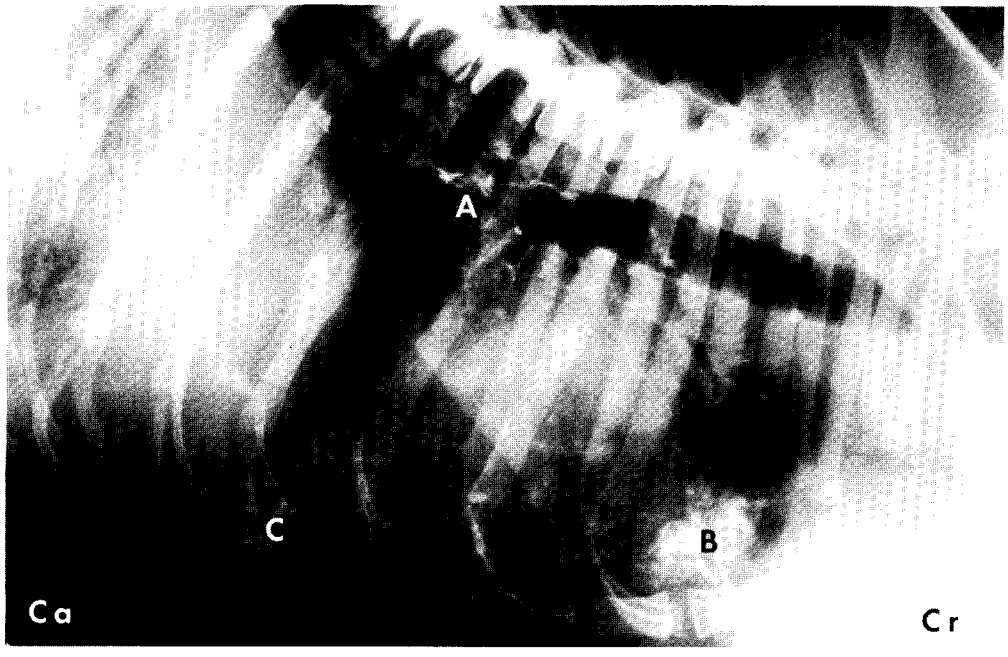

Fig. 1. Lateral X-ray of the thorax obtained 3 days after the injection of $CaWO_4$ into the pleural space. The appearance of the tungsten marker is highly distinctive and has accumulated in areas corresponding to the paravertebral costal sinus (A), parasternal lymph nodes (B) and retrocardiac mediastinal pleural folds (C). Ca=caudal; Cr=cranial.

coated by Au/Pt under vacuum and examined in a JEOL JSM-35C scanning electron microscope. The electron micrographs were derived from secondary or backscattered electrons, the latter mode being used to detect tungsten *in situ* by elemental particle analysis of the tissue preparations.

RESULTS

X-ray analysis

Lateral X-rays of the thorax showed accumulation of $CaWO_4$ particles in the paravertebral costal sinuses; parasternal lymph nodes and retrocardiac pleural folds *(Fig. 1)*. The presence of the tungsten marker in the retrocardiac pleural folds was confirmed at necropsy from day 1-7 after tungsten instillation. High resolution radiography of intrathoracic structures also showed preferential accumulation of $CaWO_4$ in the parasternal lymph nodes, parietal pleura and in lung hilar lymph nodes *(Fig. 2)*, but minimal amounts in paraaortic and subcarinal lymph nodes, the thoracic duct, visceral pleura and diaphragm *(Fig. 2)*. High magnification views of the tungsten-positive nodes showed a non-homogeneous distribution of $CaWO_4$ in the nodal tissue. In fact, tungsten deposition followed a honeycomb-like pattern, i.e., the marker appeared to encircle tungsten-free areas of tissue perhaps corresponding to nodal follicles *(Fig. 3)*.

Light microscopy

Tungsten inclusions were readily identified by light microscopy (see *Fig. 4* showing parasternal lymph node 3 days after intrapleural deposition of $CaWO_4$). The subcapsular domains of the lymph node were the first site capturing tungsten particles, as observed at days 1 and 2 after intrapleural injection *(Fig. 4)*. $CaWO_4$ was

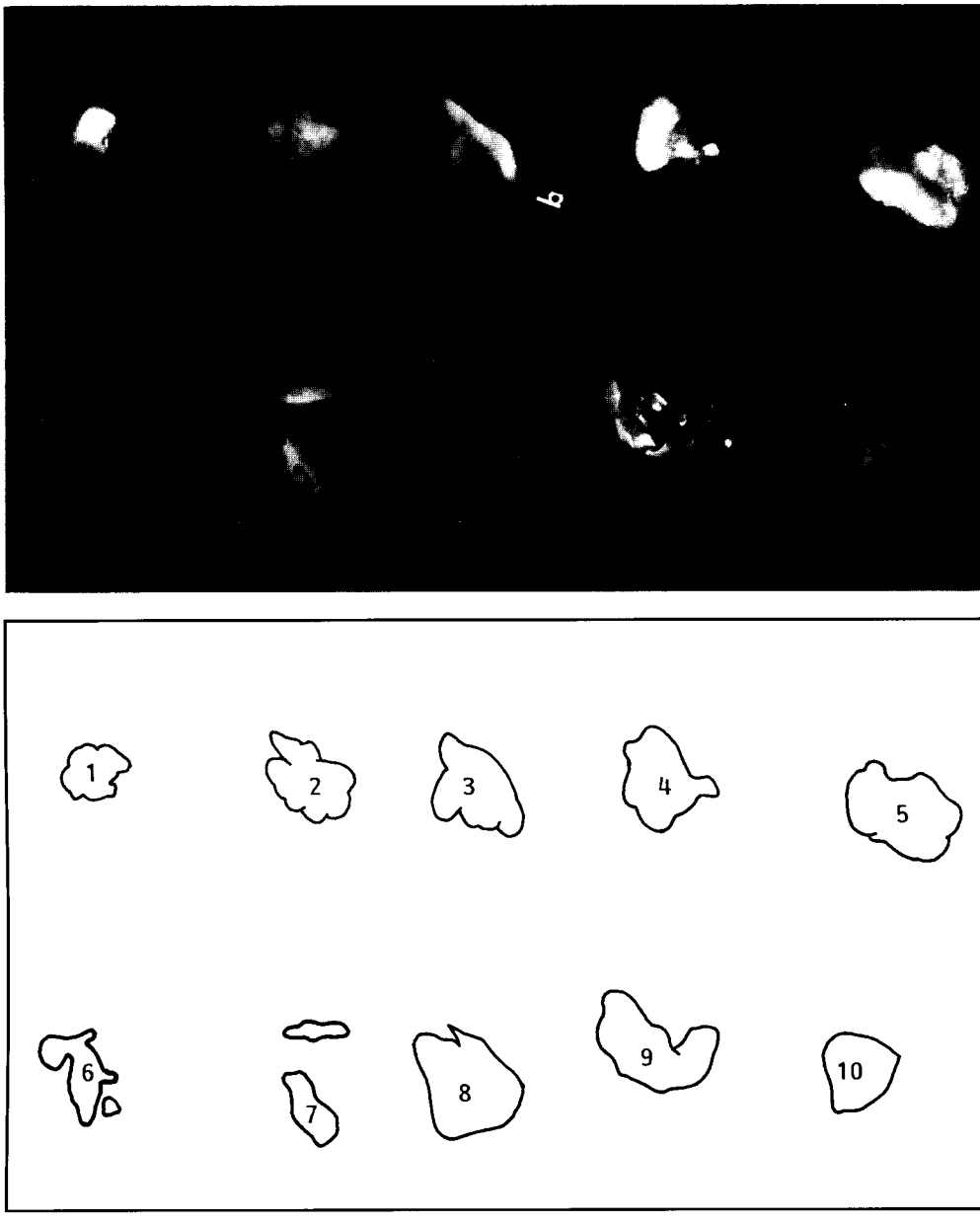

1 — Right Pulmonary Hilar Node; 2 — Subcarinal Node; 3 — Left Pulmonary Hilar Node; 4— Left Parasternal Node; 5 — Right Parasternal Node; 6 — Thoracic Duct; 7 — Para-Aortic Nodes; 8 — Diaphragm; 9 — Parietal Pleura; 10 — Visceral Pleura

Fig. 2. X-ray of nodal samples with accompanying line drawing 3 days after instillation of $CaWO_4$ into the pleural space. Tungsten is well seen in the parasternal lymph nodes and to a lesser extent in parietal pleura and hilar lymph nodes. Little or no $CaWO_4$ is seen in the thoracic duct; paraaortic nodes, diaphragm and visceral pleura.

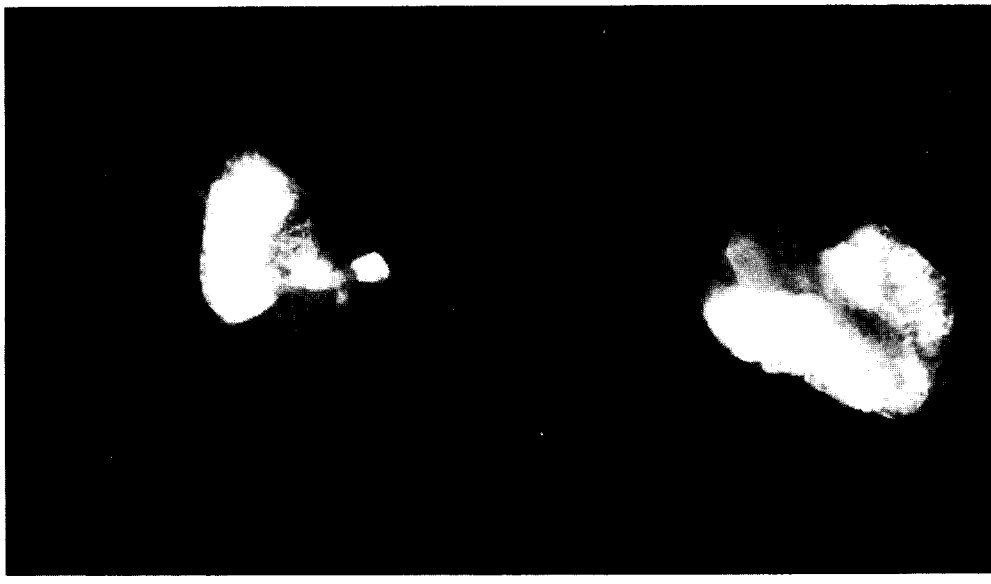

Fig. 3. Higher magnification of the parasternal nodes shown in Fig. 2 *showing the inhomogenous distribution of $CaWO_4$ apparently encircling the nodal follicles.*

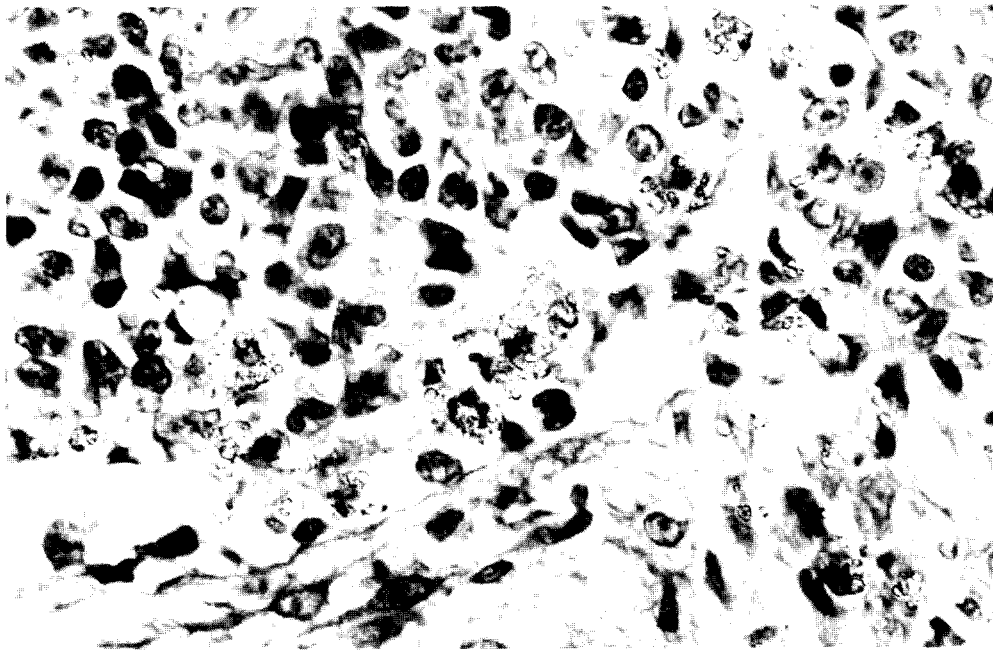

Fig. 4. Photomicrograph of parasternal lymph node collected 24 hours after the introduction of $CaWO_4$ into the pleural space. Tungsten inclusions are seen as translucent (yellow-green) inclusions. $CaWO_4$ is located in the subcapsular sinus mostly in a free form (magnification x400).

TABLE 1
Comparison of $CaWO_4$ Amounts in Six Different Intrathoracic Lymph Node Sites After Deposition of $CaWO_4$ into the Pleural Space

DAY	RPH	LPH	RPS	LPS	PAN	SCN
1	+	+	+++	+++	0	+
2	+	+	+++	+++	0	+
3	++	++	++++	++++	0	++
5	+++	++	+++	+++	+	+++
7	+++	+++	+++	+++	++	+++

RPH=right pulmonary hilar node; LPH=left pulmonary hilar node; RPS=right parasternal node; LPS=left parasternal node; PAN=para-aortic nodes; SCN=subcarinal node

also free in the extracellular space at days 1 and 2. Later (days 2 to 7) $CaWO_4$ permeated other histological domains of the lymph nodes, but seemingly spared the follicular zones. Rather, tungsten encircled the follicles, a finding in accordance with X-ray analysis of the lymph nodes (vida supra). At one week, tungsten inclusions were spread throughout the whole lymph nodal tissue. This sequence was most evident in the parasternal lymph nodes.

Semiquantitative assessment of the tungsten deposition in the different thoracic lymph nodal subgroups *(Table 1)* indicated that parasternal lymph nodes initially received substantial amounts of $CaWO_4$ with a peak of tungsten deposition at day 3. By day 3, tungsten was also detected, albeit in moderate amounts, in pulmonary hilar and subcarinal nodes. Between day 3 and day 7, tungsten deposition decreased in the parasternal nodes and increased in the pulmonary hilar and subcarinal nodes. Paraaortic nodes showed tungsten deposits only at 7 days after intrapleural instillation of $CaWO_4$.

Scanning electron microscopy (SEM)

By coupling X-ray elemental analysis to the SEM apparatus we confirmed that the inclusions identified as tungsten particles by light microscopy corresponded to elemental tungsten. The general features of tungsten distribution in lymph nodal zones as described for light microscopy were verified by SEM.

DISCUSSION

We chose $CaWO_4$ as a particle marker because it is water-insoluble, non-antigenic and an exceedingly rare component of the normal breathing atmosphere. Moreover, this particulate is composed of tetragonal crystals that are small enough (less than 10μ) to be absorbed by the pleural lymphatics. $CaWO_4$ is also readily identifiable by light microscopy because of its autofluorescence and refringency (expressed by a yellow-green color) and can be specifically identified by scanning electron microscopy as elemental tungsten. Finally, $CaWO_4$ is a heavy metal salt readily detectable by X-ray analysis.

After instillation of $CaWO_4$ into the pleural space, there were specific kinetics and pathways for particulate clearance. Initially, parasternal lymph nodes received the tungsten powder as well as milky spots of the retrocardiac pleural folds. After 3 days a general permeation of several lymph node groups occurred during this second phase of particle clearing. Accumulation of the tungsten marker in the paravertebral costal sinuses, parasternal lymph nodes and retrocardiac pleural folds (demonstrated by presacrifice X-ray) confirmed a distribution

pattern described previously in the dog using a radiolabeled marker (10). The localization pattern of the tungsten marker favored the existence of powerful absorptive processes in these sites (11,12), that is, in the dependent areas of the pleural cavity and in the extracostal regions (2).

Clearance of calcium tungstate particles from the pleural space of the dog is relatively rapid (day 1 and even by 12 hours), and initially is primarily into the parasternal lymph nodes, suggesting that this lymph nodal subgroup is a major absorption site for the pleural space (periods before 12 hours were not examined). This rapid absorption of pleural particles is in contrast with the observations of Courtice and Simmonds (7) who maintain that particle clearance from the pleural space is via the mediastinal pleura, a site which drains to the pulmonary and tracheobronchial lymph nodes (13). The rapidity of pleural particulate absorption is probably related to the large concentration of lymphatic vessels in the parietal pleura, and also to the existence of specialized mesothelial and diaphragmatic structures (i.e., stomas and milky spots that vigorously transport intrapleural particles) (14-18).

The rapid kinetics of $CaWO_4$ particle clearance from the pleural space is in distinct contrast to the slow absorption of $CaWO_4$ particles from the bronchoalveolar space into regional lymph nodes. The slowness of the latter phenomenon is probably attributable to the paucity of lymphatics in the alveolar membrane (9). At 24 hours after intrapleural particle injection, $CaWO_4$ appears in the marginal sinuses of the parasternal lymph nodes chiefly in the extracellular space. From day 3 to day 7, the particles are subsequently seen inside cells of the follicular area of the outer cortex, in the paracortex and finally inside the follicular domains of the lymph node. This nodal distribution of tungsten conforms with previous findings in popliteal nodes after injection of carbon particles under the skin of sheep (19). By day 7 after pleural space instillation, tungsten particles permeate all zones of the lymph node. Some $CaWO_4$ particles are located inside macrophages, suggesting transport by phagocytes from the non-follicular regions (i.e., marginal, interfollicular and medullary domains) where $CaWO_4$ is first identified in the follicles.

Semiquantitative analysis *(Table 1)* indicated that by day 3 several intrathoracic lymph node subgroups contained different amounts of absorbed tungsten. By day 7, however, tungsten was evenly distributed among all the intrathoracic lymph node subgroups. Of interest, dissemination of $CaWO_4$ within the thorax was accompanied by a notable decrease in tungsten in the parasternal lymph nodes suggesting that after day 3 further absorption and dissemination of the tungsten marker originated from this nodal subgroup. This interpretation differed with earlier work (7,13), which suggested that subcarinal and pulmonary hilar nodes were the primary lymph nodal drainage pathway of the mediastinal pleura. Our data were more in accordance with the interrelated network model of the intrathoracic lymph circulation as proposed by von Hayek (20). A small component of $CaWO_4$ can also reach the hilar nodes via the lung parenchyma (5,6).

Identification of tungsten particles in retrocardiac pleural folds as early as 24 h after $CaWO_4$ instillation into the pleural space, suggests a key role of these folds in the local mechanisms of host defense. The pleural cavity is efficient in the clearing of exogenous agents, a phenomenon previously attributed to the presence of milky spots in the lower mediastinum (16,21). Milky spots were first described by von Recklinghausen (22) in the rabbit and represent a capillary network surrounded by an aggregate of macrophages, lymphocytes, and plasma cells (23). These milky spots are uniformly observed in the retrocardiac pleural folds of the dogs studied suggesting that in the canine they are distributed similarly to that in the rabbit (22) and in the white rat (16). The appearance of the tungsten marker as earlier as 24 h after pleural space instillation in the milky spots (well seen in necropsy) suggests that milky spots are also pivotal to efficient clearance from the pleural space.

The nature of milky spot cellular composition also implies that they have an important immunologic role in the overall intrathoracic defense mechanisms of the host (24) and similar to that proposed for milky spots of the greater omentum (25).

In conclusion: 1) the clearance of particles from the pleural space into regional lymph nodes is much faster than bronchoalveolar particulate clearance; 2) milky spots of pleural folds are important contributors to the clearance of exogenous particles; 3) the parasternal lymph node subgroup is initially the chief drainage pathway for intrapleural particles; and 4) essentially all thoracic lymph nodal subgroups ultimately receive exogenous particles introduced into the pleural space.

ACKNOWLEDGMENTS

The authors thank Dr. Artur Águas for his collaboration in the text revision and permanent constructive advice. The technical assistance of A. Ribeiro, Costa e Silva, E. Monteiro, J. Aurélio, A. Lagrifa, and L. Nogueira is also gratefully acknowledged.

REFERENCES

1. Daniele, RP: The pleura in local and systemic immune disorders. In *The Pleura in Health and Disease,* Chr*tien, J, J Bignon, A Hirsch (Eds.), New York, Dekker, 1985, 369-383.
2. Miserocchi, G: Pleural pressures and fluid transport. In: *The Lung: Scientific Foundations.* Crystal, RG, JB West, PJ Barnes, et al (Eds.), New York, Raven Press, 1991, 885-893.
3. Zocchi, L, E Agostoni, D Cremaschi: Electrolyte transport across the pleura of rabbits. Respir. Physiol. 86 (1991), 125-138.
4. Burke, HE: The lymphatics which drain the potential space between the visceral and the parietal pleura. Am. Rev. Tuberc. 79 (1959), 52-65.
5. Pereira, AS, N Grande, A Ribeiro, et al: Experimental study of clearance of particles from the pleural space. Surg. Rad. Anat. 13-2 (1991), 27S.
6. Pereira, AS, N Grande, E Carvalho, et al: Evidence of drainage of tungsten particles introduced in the pleural space through the visceral pleura into the lung parenchyma. Acta Anatomica (1992) (in press).
7. Courtice, FC, WJ Simmonds: Physiological significance of lymph drainage of the serosal cavities and lungs. Physiol. Rev. 34 (1954), 419-448.
8. Hagiwara, A, T Takahashi: A new drug delivery system of anticancer agents: Activated carbon particls adsorbing anticancer agents. In Vivo 1 (1987), 241-252.
9. Grande, NR, CM Sá, AP Águas, et al: Time course and distribution of tungsten laden macrophages in the hylar lymph nodes of the dog lung after experimental instillation of calcium tungstate into the left apical bronchus. Lymphology 23 (1990), 171-182.
10. Miserocchi, G, M Pistolesi, M Miniati, et al: Pleural liquid pressure gradients and intrapleural distribution of injected bolus. J. Appl. Physiol. Respirat. Environ. Exercise Physiol. 56-2 (1984), 526-532.
11. Miserocchi, G, E Mariani, D Negrini: Role of the diaphragm in setting liquid pressure in serous cavities. Respir. Physiol. 50 (1982), 381-392.
12. Miserocchi, G, T Nakamura, E Mariani, et al: Pleural liquid pressure over the interlobar mediastinal and diaphragmatic surfaces of the lung. Respir. Physiol. 46 (1981), 61-69.
13. Kim, KJ, AM Critz, ED Crandall: Transport of water and solutes across sheep visceral pleura. Am. Rev. Respir. Dis. 120 (1979), 883-892.
14. Wang, NS: The preformed stomas connecting the pleural cavity and the lymphatics in the parietal pleura. Am. Rev. Respir. Dis. 111 (1975), 12-20.
15. Maximow, AA: Relation of blood cells to connective tissue and endothelium. Physiol. Rev. 4 (1924), 533-563.
16. Corray, GH: Defensive mechanisms in the mediastinum, with special reference to the mechanics of pleural absorption. J. Pathol. Bacteriol. 61 (1949), 551-567.
17. Burke, HE: The lymphatics which drain the potential space between the visceral and the parietal pleura. Am. Rev. Tuberc. 79 (1959), 52-65.
18. Choné, B: Mesotheliale radiogold-inkorporation im submikroskopischen bild. Fortschr. Roentgenstr. 105 (1966), 566-578.
19. Heath, TJ, R Kerlin, H Spalding: Afferent pathways of lymph flow within the popliteal node in sheep. J. Anat. 149 (1986), 65-75.

20. von Hayek, H: *Die Menschliche Lunge. 2. Erganzte und Erweitert Auflage.* Berlin, Springer-Verlag, 1970.
21. Hirsch, A, JF Bernaudin, M Nebut, et al: Le mesothelium pleural: Structure et fonctions. Bull. Eur. Physiopathol. Respir. 12 (1976), 387-406.
22. von Recklinghausen, F: Uber Eiter-Bindegewebskorperchen. Virchows Arch. Pathol. Ana. 28 (1863), 157-166.
23. Carr, I: The fine structure of the cells of the mouse peritoneum. Z. Zellforsch. 80 (1967), 534-555.
24. Kanazawa, K: Exchanges through the pleura-cells and particles. In: *The Pleura in Health and Disease.* Chrétien, J, J Bignon, A Hirsch (Eds.), Marcell Dekker, Inc., New York, 1985, 195-231.
25. Shimotsuma, M, M Kawata, A Hagiwara, et al: Milky spots in the human greater omentum—Macroscopic and histological identification. Acta Anat. 136 (1989), 211-216.

Nuno R. Grande, M.D., Ph.D.
Sector de Morfologia Normal
Instituto de Ciencias Biomédicas
Abel Salazar
Largo Prof. Abel Salazar, 2
4000 Porto, PORTUGAL